SCIENTIFIC REPORTS

OPEN

SUBJECT AREAS:
ELECTRONIC DEVICES
MAGNETIC PROPERTIES AND MATERIALS
ELECTRONIC PROPERTIES AND MATERIALS

Received
29 July 2014

Accepted
13 October 2014

Published
12 November 2014

Correspondence and requests for materials should be addressed to H.-C.W. (wuhc@tcd.ie) or M.A. (moabid@ksu.edu.sa)

Magnetic and transport properties of epitaxial thin film $MgFe_2O_4$ grown on MgO (100) by molecular beam epitaxy

Han-Chun Wu[1,2], Ozhet Mauit[3], Cormac Ó Coileáin[2,3], Askar Syrlybekov[3], Abbas Khalid[3], Anas Mouti[2], Mourad Abid[2], Hong-Zhou Zhang[3], Mohamed Abid[2] & Igor V. Shvets[3]

[1]School of Physics, Beijing Institute of Technology, Beijing, 100081, P. R. China, [2]KSU-Aramco Center, King Saud University, Riyadh 11451, Saudi Arabia, [3]CRANN, School of Physics, Trinity College, Dublin 2, Ireland.

Magnesium ferrite is a very important magnetic material due to its interesting magnetic and electrical properties and its chemical and thermal stability. Here we report on the magnetic and transport properties of epitaxial $MgFe_2O_4$ thin films grown on MgO (001) by molecular beam epitaxy. The structural properties and chemical composition of the $MgFe_2O_4$ films were characterized by X-Ray diffraction and X-Ray photoelectron spectroscopy, respectively. The nonsaturation of the magnetization in high magnetic fields observed for M (H) measurements and the linear negative magnetoresistance (MR) curves indicate the presence of anti-phase boundaries (APBs) in $MgFe_2O_4$. The presence of APBs was confirmed by transmission electron microscopy. Moreover, post annealing decreases the resistance and enhances the MR of the film, suggesting migration of the APBs. Our results may be valuable for the application of $MgFe_2O_4$ in spintronics.

Spinel ferrites, of the general formula MFe_2O_4 (M = Mn, Co, Ni, Mg, or Zn), have recently attracted considerable attention due to their interesting magnetic and electrical properties with enhanced chemical and thermal stability[1–3]. Among them, magnesium ferrite ($MgFe_2O_4$) is a soft magnetic *n*-type semiconductor with a partially inverse spinel structure. It has high sensitivity, good chemical stability, and its band gap of ~ 2.0 eV makes it a suitable candidate for a wide range of applications in heterogeneous catalysis, adsorption, sensors, organic pollutants, lithium-ion batteries, and photoelectrochemical water splitting[4–8]. Moreover, it has a high Curie temperature, adding it as a potential candidate in spintronics. So far, most studies have focused on $MgFe_2O_4$ nanoparticles[4–8] or nanopillars[9]. However, less attention has been paid to epitaxial $MgFe_2O_4$ thin films although they are of great interest from both fundamental and practical perspectives. There have been relatively few attempts to grow $MgFe_2O_4$ thin films using pulsed laser deposition (PLD)[10,11] or molecular beam epitaxy (MBE)[12,13]. None of them studied the effects of natural growth defects on the transport properties, such as anti-phase boundaries, which are expected to be common in oxide-based nanoelectronic and spintronic devices.

In this paper, we report on the magnetic and transport properties of epitaxial $MgFe_2O_4$ thin films grown on MgO (001) substrates by molecular beam epitaxy. The structural properties and chemical composition of the $MgFe_2O_4$ films were characterized by high resolution X-ray diffraction (XRD) and X-ray photoemission spectroscopy (XPS), respectively. The magnetic and transport properties were investigated using a physical property measurement system (PPMS). We observed a large non-saturated field and a negative linear magnetoresistance (MR) due to the presence of anti-ferromagnetic (AF) anti-phase boundaries in the $MgFe_2O_4$. The presence of the APBs was clearly verified by high resolution scanning transmission electron microscopy (HRSTEM) characterization. Moreover, our results also suggest that post annealing can cause migration of the APBs, which decreases the resistance and enhances the MR of the film.

Results

Sample preparation and characterization. $MgFe_2O_4$ thin films, with different thicknesses, were grown on (100) oriented MgO single crystal substrates in an oxygen–plasma-assisted molecular beam epitaxy (MBE) system. The base pressure of the system is better than 5×10^{-10} Torr. The substrates were chemically cleaned prior to insertion into the growth chamber and then cleaned *in situ* by annealing at 600°C in ultra-high vacuum

(UHV) for 1/2 hour followed by further annealing in 1×10^{-5} Torr oxygen for 2 hours. Co-deposition was used to grow the thin films, i.e., material fluxes were produced by e-beam evaporation of separate pure MgO and metallic Fe sources. The growth rates for Fe and MgO were set to 0.6 Å/s and 0.3 Å/s, respectively. During growth, the substrate temperature was maintained at 300°C and the plasma source was operated with an oxygen partial pressure of 2×10^{-5} Torr and a current of 30 mA. After deposition, the samples were annealed at 300°C, with the same oxygen partial pressure, for 3 hours. Reflection high energy electron diffraction (RHEED) was employed to establish the growth mode. RHEED patterns for the MgO substrate and $MgFe_2O_4$ thin films (Fig. 1a and 1b) show vertical lattice rods and sharp Kikuchi lines, representative of a well-ordered and smooth surface, demonstrating the epitaxial growth of the $MgFe_2O_4$ films on MgO substrates. The structural properties and chemical composition were further investigated using a high resolution XRD system and XPS. Figure 1c shows the full range XRD, from 10 to 100 degrees, for a 114 nm thick $MgFe_2O_4$ film on a MgO substrate. Only the (200) and (400) peaks for the MgO substrate and the (008) and (004) peaks for the $MgFe_2O_4$ film are observed indicating the epitaxial growth of the $MgFe_2O_4$. The peak positions for MgO (400) and $MgFe_2O_4$ (008) located at 93.88° and 94.47° respectively, which are consistent with the well-established values. X-ray photoemission spectroscopy compositional analysis of the surface of the $MgFe_2O_4$ film is shown in Figure 1d. The Mg 2p and Fe 3p peaks have been consistently energy shifted to align the C 1s peak position to a binding energy (BE) of 284.7 eV. The XPS characterization indicates the atomic ratio of Mg : Fe is around 1 : 2. To investigate the interface between MgO and $MgFe_2O_4$, Figure 1e presents a low-magnification high angle angular dark field (HAADF) STEM image showing the whole thickness of a $MgFe_2O_4$ thin film (bright) on a MgO substrate (dark). The interfaces are sharp and defect free which further confirms $MgFe_2O_4$ films were epitaxially grown on the MgO substrates. A selected area electron diffraction (SAED) pattern of the interface between MgO and $MgFe_2O_4$ is shown in Fig. 1f. The red circles highlight the SAED spots for

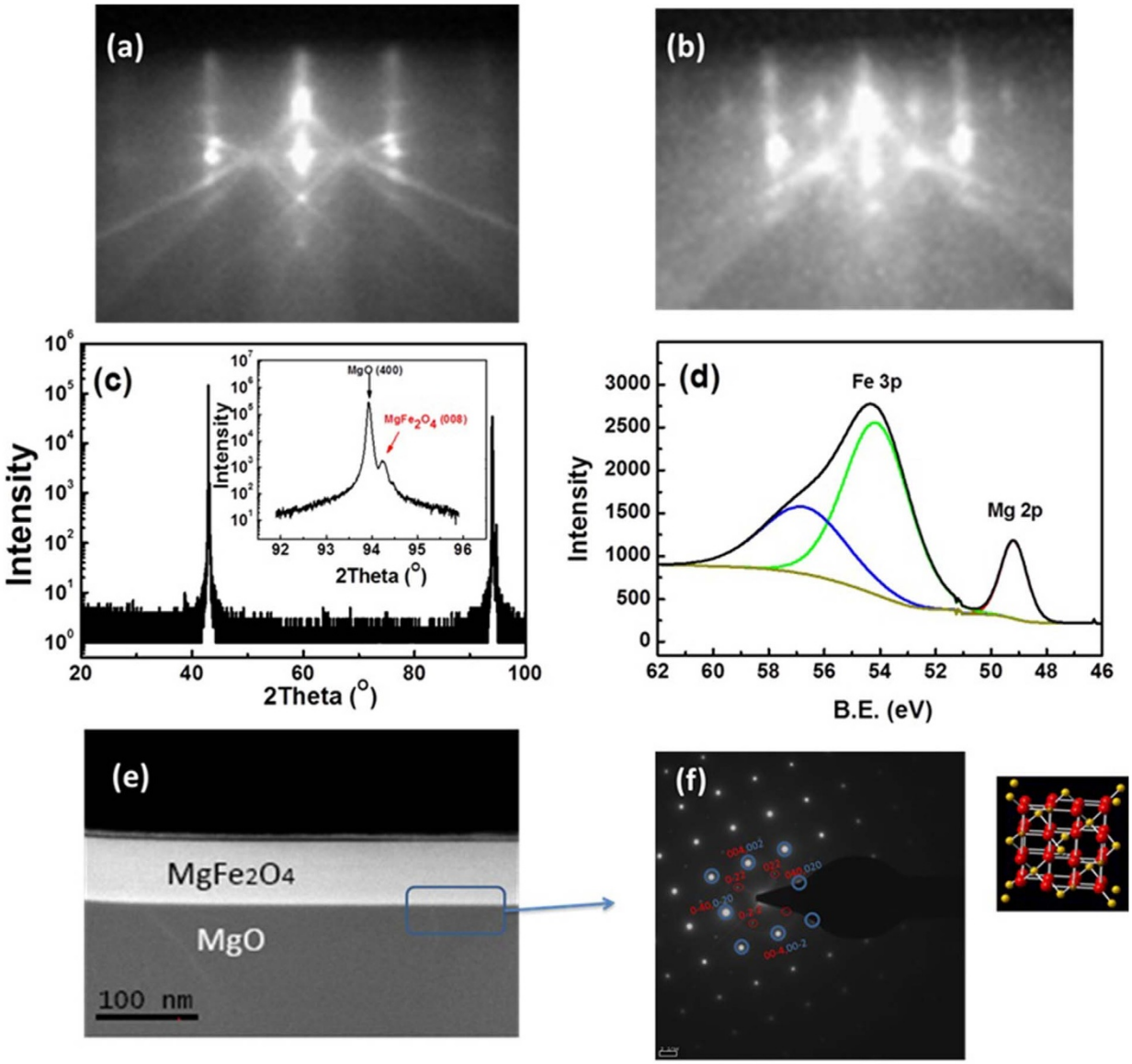

Figure 1 | RHEED images of (a) UHV annealed MgO (001) substrate and (b) 10 nm of $MgFe_2O_4$ growth on MgO, indicating the epitaxial growth of $MgFe_2O_4$. (c) XRD plot for a 114 nm thick $MgFe_2O_4$ film on a MgO substrate indicating the epitaxial growth mode. Inset in (c): XRD plot in the range from 92 to 96 degrees. (d) X-ray photoemission spectroscopy compositional analysis of the surface of the $MgFe_2O_4$ film on MgO. (e) Low-magnification HAADF image of the whole $MgFe_2O_4$ thin film (bright) on MgO substrate (dark) and (f) SAED pattern of the MgO and $MgFe_2O_4$ interface indicating the high quality of epitaxial $MgFe_2O_4$ film. Inset: Atomic structure of $MgFe_2O_4$.

$MgFe_2O_4$ only and the blue circles highlight the SAED spots for the MgO and $MgFe_2O_4$. A small lattice mismatch is observed indicating the high quality of the epitaxial thin film.

Magnetic and transport properties. The magnetic properties of the $MgFe_2O_4$ thin films were investigated by means of a PPMS (Quantum Design). Temperature dependent M (H) loops of a 114 nm thick $MgFe_2O_4$ thin film are displayed in Fig. 2a. The external magnetic field is applied in the film plane along [100] direction. It is clear that the film is ferromagnetic in nature at all the temperatures. The coercivity increases with decreasing temperature. The measured magnetization at 300 K and at 1 T is around 115 emu/cm^3, which is larger than the value reported for $MgFe_2O_4$ nano pillars[9] but smaller than the value for $MgFe_2O_4$ grown on sapphire substrates[11]. Interestingly, the magnetization does not saturate in a field of 1T for all temperatures. Figure 2b shows M (H) loops for the same 114 nm thick $MgFe_2O_4$ thin film measured at room temperature with the external magnetic field applied along [100] and [110] directions. A significant difference between the M (H) loops for the two field directions is clearly observed. At room temperature, for a 114 nm thick $MgFe_2O_4$ thin film, with the field along the [100] direction, the coercivity field is 127 Oe. While when the field is along the [110] direction, the coercivity field increases to 216 Oe. Moreover, the M (H) loop for the field along [110] is much squarer than for field applied along [100]. It is clear that the easy axis, for the films grown, is along the [110] direction and hard axis is along the [100] direction. Figure 3a shows the magnetoresistance curves of a 114 nm thick $MgFe_2O_4$ thin film on a MgO substrate measured at different temperatures, where MR is defined as MR=R(H)/R(0)-1. The transport properties of $MgFe_2O_4$ were measured using the conventional four-probe method in the PPMS (Inset of Fig. 3a). A bias current of 4 μA was applied between the two outer contact electrodes along the [100] direction of the MgO substrate and a Keithley 2400 was used to measure the voltage drop. The external field was applied along the current direction. From Figure 3a, one can clearly see that the resistance shows a linear response to the external field at all temperatures. The MR ratio as a function of temperature is summarized in Figure 3b. It should be noted that the MR ratio increases with decreasing temperature. A MR ratio of −0.55% was obtained at room temperature and a MR of −3% was achieved at 80K. We would like to mention here that the shape of the MR curves is independent of temperature.

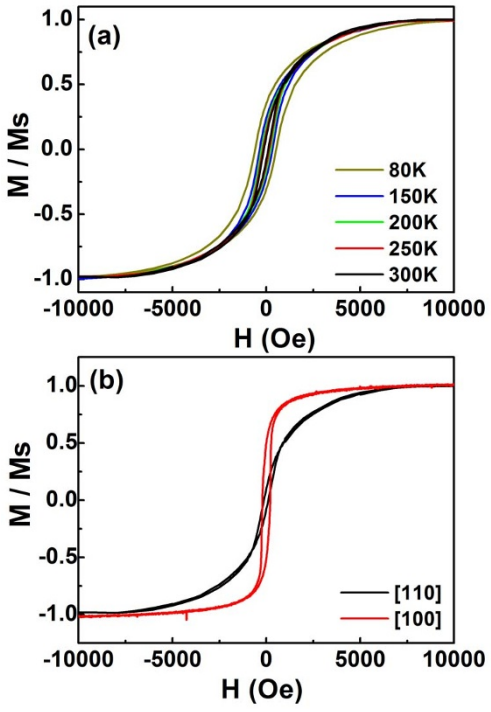

Figure 2 | (a) M (H) loops of a 114 nm thick $MgFe_2O_4$ film measured at different temperatures with an in-plane magnetic field applied along the [100] direction. (b) M (H) loops of a 114 nm thick $MgFe_2O_4$ film measured at room temperature with an in-plane magnetic field applied along the [100] and [110] directions.

Discussion

Presence of APBs. The observed very large saturation field and negative linear MR can be attributed to and explained by the presence of antiphase boundaries, which are natural defects occurring during growth. The existence of APBs has been verified in numerous systems, for example, magnetite on MgO substrates[14–22], $Ba_{0.6}Sr_{0.4}TiO_3$ on (001) MgO[23], Ba(Zr,Ti)O_3 on (001) MgO[24], and etc. The reported anti-phase boundaries in epitaxial Fe_3O_4 films grown on MgO substrates is a consequence of lattice parameter of Fe_3O_4 (8.397 Å) being almost twice of that of the MgO substrate (4.213 Å), and its spinel structure being of lower symmetry (Fd3m) than that of MgO (Fm3m). The presence of these APBs defects in Fe_3O_4 contributes to unusual magnetic and transport properties, such as the magnetization non-saturation even at very high field[14,15], super-paramagnetic behavior in Fe_3O_4 films[16,17], miscompensation of the spin moments at the surface and at the APBs contribute a giant magnetization[18], a greater MR response across the AF-APBs[19–21], and a large transversal MR[22]. Similar to Fe_3O_4, $MgFe_2O_4$ has a lattice parameter of (8.38 Å) and its spinel structure is of lower

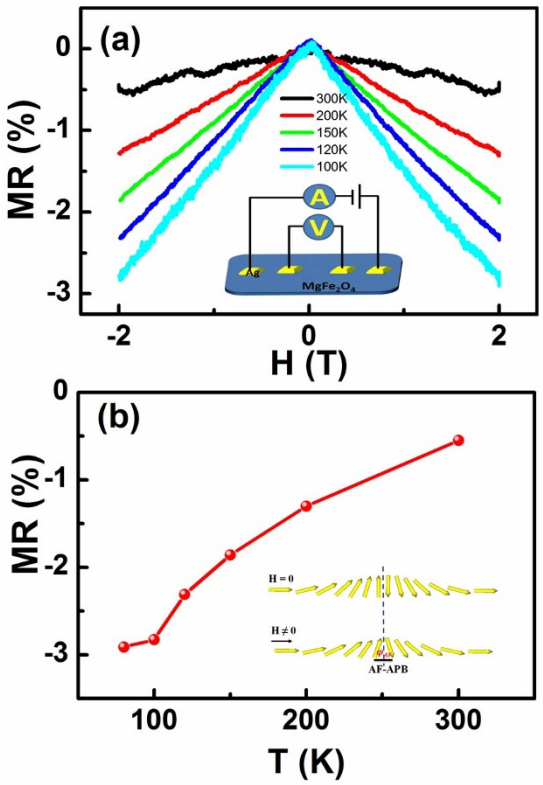

Figure 3 | (a) MR curves for a 114 nm thick $MgFe_2O_4$ film after annealing with oxygen for 3 hours, measured at different temperatures. The magnetic field is applied in the film plane along the [100] direction. Inset: Schematic drawing of the setup used to measure the MR. (b) MR ratio as a function of temperature under a field of 2T. Inset: Schematic drawing of spin structure disturbance due to an AF-APB with and without an in-plane external field.

symmetry (Fd-3m). Therefore APBs are expected to form during growth of $MgFe_2O_4$ on MgO. To confirm the existence of the APBs, we show in Figure 4a a dark field cross-sectional HRTEM image of a 114 nm $MgFe_2O_4$ thin film on a MgO substrate. Several APBs are clearly visible. To highlight their presence, some APB domains are marked with dotted blue lines. Notably, $MgFe_2O_4$ is a partially inverse spinel. Thus, the spin configuration for atoms separated across APBs will be in a non-collinear configuration which means the spin states will be at least partially antiparallel. Therefore, the observed very large saturation field and negative linear MR in $MgFe_2O_4$ can be explained by the presence of AF-APBs. APB induced MR has been also observed in $Ba_{0.6}Sr_{0.4}TiO_3$[23] and $Ba(Zr,Ti)O_3$[24] films on MgO substrates. As can be done for Fe_3O_4, we schematically drew the spin structure disturbance due to the presences of AF-APBs, with and without an in-plane external field, as the inset of Figure 3a. The external field aligns the spins far from the boundary and the spins at the APBs rotate by an angle of φ_{AF} (marked in the inset of Figure 3b), where φ_{AF} is the angle between the spins at the left side of the APB and the external field. We can write the conductivity of the film as $\sigma = \sigma_0 + t_0^2 \cos^2\varphi_{AF}$, where σ_0 is due to spin-dependent scattering at the interface without an external field and the second term is dependent on the MR effect[21]. The MR ratio for $MgFe_2O_4$ is around half that for Fe_3O_4, for the same thickness, indicating the AF APBs in $MgFe_2O_4$ are not as sharp as those in Fe_3O_4 and the exchange stiffness for the AF exchange interaction at the boundaries is not as strong as for Fe_3O_4. The underlying reason is that $MgFe_2O_4$ is a partially inverse spinel. φ_{AF} may not be zero in the absence of an external field. According to Ref. 14, the equation $M = Ms\ (1\text{-}b/H^n)$ can be used to describe the approach towards saturation, of the magnetization (M) as a function of field, a value for the exponent (n) near 0.4 was obtained for $MgFe_2O_4$. This value is smaller than that for Fe_3O_4 (0.5) but it is almost the same as for $NiFe_2O_4$ films[25].

To study effect of strain on APB formation, we prepared 4 sets of $MgFe_2O_4$ films in different strain states. The thicknesses of those 4 sets of $MgFe_2O_4$ films are around 114 nm (S1), 100 nm (S2), 90 nm (S3), and 60 nm (S4), respectively. Figure 4b shows XRD spectra for those 4 sets of $MgFe_2O_4$ films. To calculate the strain for those films, first the out-of-plane lattice constant $a_\perp$ is calculated with $a_\perp = d_{hkl}\sqrt{h^2+k^2+l^2} = \frac{n\lambda}{2\sin\theta}\sqrt{h^2+k^2+l^2}$, where d_{hkl} is the spacing of lattice planes with the Miller indices (hkl), θ is the corresponding Bragg angle of the films, λ the wavelength of X-rays used, and n is an integer. The calculated out-of-plane lattice constants $a_\perp$ are 8.379 Å (S1), 8.377 Å (S2), 8.373 Å (S3), and 8.368 Å (S4), respectively. Thus, the corresponding strains for the films (e) are 0.1%, 0.07%, 0.03%, and 0.004%, respectively, which can be calculated from $e = \frac{a_0 - a_\perp}{a_0}$. Where a_0 is the lattice constant of $MgFe_2O_4$ (8.38 Å). Figure 4c shows R-T curves for those 4 sets of $MgFe_2O_4$ films. The resistivity of the films decreases with decreasing strain. The underline physics is that the APB domain size increases with decreasing strain. To confirm this, we estimated the APB domain size δ from the XRD data using $\delta = 0.9\lambda/(B\cos\theta)$, where B is the half-width value of the XRD peaks. The estimated APB domain sizes for those 4 sets of $MgFe_2O_4$ films are 12 nm, 18 nm, 21 nm, and 29 nm, respectively. The strain as a function of grain size is summarized in Fig. 4d. One can see that with decreasing the strain, the APB domain size increases which results in the decrease in the resistivity.

Effect of post annealing on electrical properties of $MgFe_2O_4$. To investigate the effect of post annealing, in the presence oxygen, on the

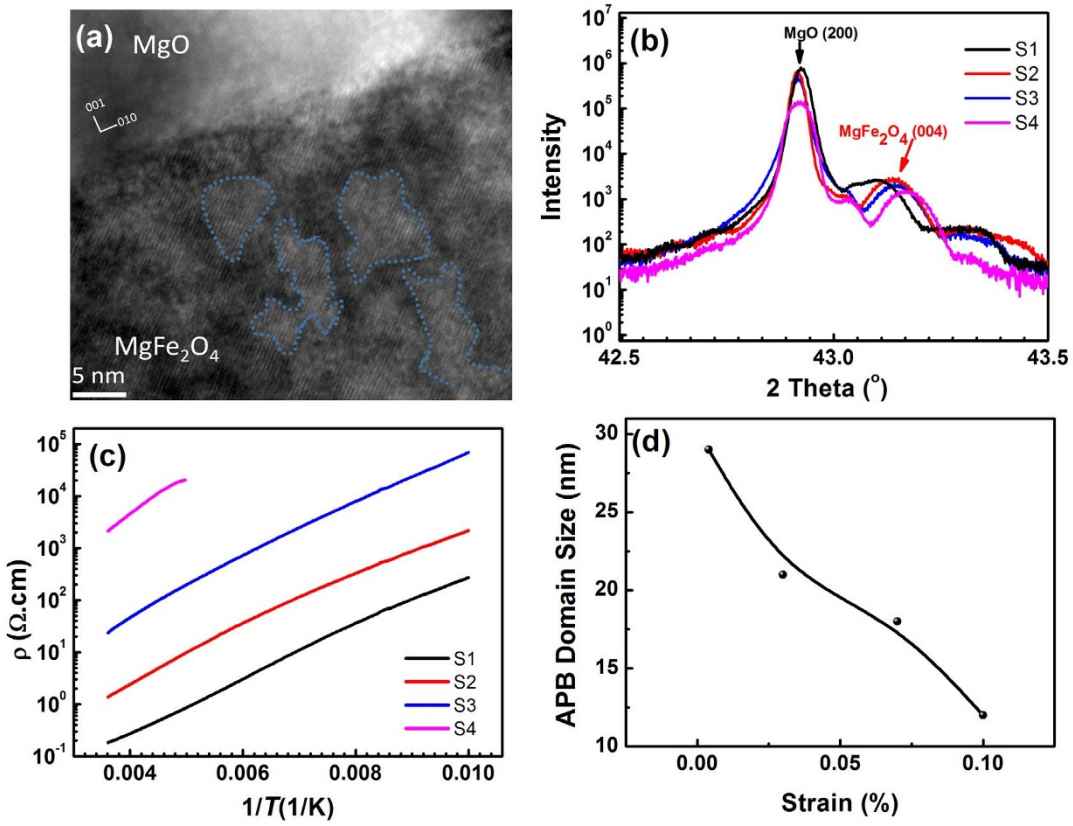

Figure 4 | (a) Dark field HRTEM image of a 114 nm thick $MgFe_2O_4$ film on a MgO substrate after annealing with oxygen for 3 hours to demonstrate the presence of APBs. (b) XRD spectra and (c) R-T curves for 4 sets of $MgFe_2O_4$ films in different strain states. (d) APB domain sizes as a function of strain.

electrical properties of $MgFe_2O_4$ films, Figure 5a shows R-T curves for an as-grown 114 nm thick $MgFe_2O_4$ film (black line) and after annealing in an oxygen partial pressure of 2×10^{-5} Torr at 300°C for 3 hours (red line). Post annealing significantly decreases the resistance of the samples. At room temperature, the resistance for an as-grown sample was 5200 Ω which decreased to 2600 Ω after annealing. Post annealing also reduces the activation energy (E_a) of the sample. The R-T plots were fitted with the relationship $R(T) \approx R_0 \exp\left(\frac{-E_a}{K_B T}\right)$. The activation energies for the as-grown sample and the sample after annealing were 76.4 meV and 67.1 meV, respectively. We also measured the MR of the as-grown $MgFe_2O_4$ sample (Figure 5b). It was found that post annealing also increases the MR ratio. The effect of post annealing can be understood as follows. First, the APBs in $MgFe_2O_4$ may migrate during annealing. It has been shown in Fe_3O_4 that post annealing at 300°C is sufficient to cause the migration of the APBs[26] which increases the APB domain size and decreases the resistance and activation energy of the films[21]. Therefore, it is reasonable to believe that APBs in $MgFe_2O_4$ can also migrate during annealing. Figure 5c shows XRD data for the as-grown 114 nm thick $MgFe_2O_4$ film (black line) and after annealing in an oxygen partial pressure of 2×10^{-5} Torr at 300°C for 3 hours (red line). The half-width value of the $MgFe_2O_4$ peak decreases after annealing, indicating an increase in the APB domain size. Another possible reason is that post annealing may modify the oxygen vacancies and nanodomain structures in $MgFe_2O_4$ which also will affect the resistivity and MR of the sample[27,28].

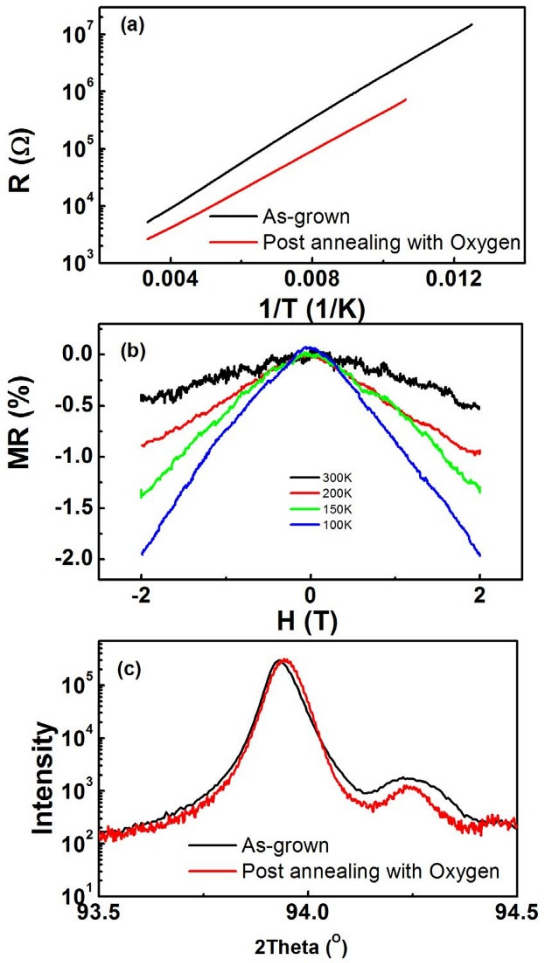

Figure 5 | (a) R-T curves and (c) XRD spectra for a 114 nm thick as-grown $MgFe_2O_4$ film (black line) and after annealing in oxygen condition for 3 hours (red line). (b) MR curves for the same as-grown 114 nm $MgFe_2O_4$ measured at different temperatures.

In summary, we investigated the magnetic and transport properties of epitaxial $MgFe_2O_4$ thin films grown on MgO (001) substrates. Large saturation fields and a linear negative MR were observed indicating the presence of APBs in $MgFe_2O_4$. The existence of APBs was further directly confirmed by HRSTEM characterization. The migration of APBs was also discussed. Our results may be valuable for the future application of $MgFe_2O_4$ in spintronics.

Methods

$MgFe_2O_4$ thin films with different thicknesses were grown on MgO (100) oriented single crystal substrates using an oxygen–plasma-assisted molecular beam epitaxy system. Co-deposition was used to grow the thin films. $MgFe_2O_4$ films in different strain states were prepared by controlling the film thickness. The magnetic and transport properties were examined by means of a physical property measurement system (PPMS, Quantum Design). X-ray photoelectron spectrometry measurements were performed in an Omicron Nanotechnology Spectroscopy system equipped with an Ar ion miller in the preparation chamber.

1. Xiang, X., Fan, G., Fan, J. & Li, F. Porous and superparamagnetic magnesium ferrite film fabricated via a precursor route. *J. Alloy Comp.* **499**, 30 (2010).
2. Bárcena, C. *et al.* Zinc ferrite nanoparticles as MRI contrast agents. *Chem. Commun.* **19**, 2224 (2008).
3. Bao, N. *et al.* Controlled Growth of Monodisperse Self-Supported Superparamagnetic Nanostructures of Spherical and Rod-Like $CoFe_2O_4$ Nanocrystals. *J. Am. Chem. Soc.* **131**, 12900 (2009).
4. Hamdeh, H. H. *et al.* Magnetic properties of partially-inverted zinc ferrite aerogel powders. *J. Appl. Phys.* **81**, 1851 (1997).
5. Busca, G., Finocchio, E., Lorenzelli, V., Trombetta, M. & Rossini, S. A. IR study of alkene allylic activation on magnesium ferrite and alumina catalysts. *J. Chem. Soc. Faraday Trans.* **92**, 4687 (1996).
6. Su, N. R. *et al.* Fabrication of $MgFe_2O_4$–ZnO heterojunction photocatalysts for application of organic pollutants. *Mater. Lett.* **122**, 201 (2014).
7. Pan, Y. *et al.* $MgFe_2O_4$ nanoparticles as anode materials for lithium-ion batteries. *Electrochimica Acta* **109**, 89 (2013).
8. Hou, Y., Zuo, F., Dagg, A. & Feng, P. Three-Dimensional Branched Cobalt-Doped a-Fe_2O_3 Nanorod/$MgFe_2O_4$ Heterojunction Array as a Flexible Photoanode for Efficient Photoelectrochemical Water Oxidation. *Angew. Chem. Int. Ed.* **52**, 1248 (2013).
9. Kim, D. H., Aimon, N. M., Sun, X. & Ross, C. A. Compositionally Modulated Magnetic Epitaxial Spinel/Perovskite Nanocomposite Thin Films. *Adv. Funct. Mater.* **24**, 2334 (2014).
10. Kim, K. S. *et al.* Influence of oxygen partial pressure on the epitaxial $MgFe_2O_4$ thin films deposited on $SrTiO_3$ (1 0 0) substrate. *J. Alloy Comp.* **503**, 460 (2010).
11. Gupta, R. K. & Yakuphanoglu, F. Epitaxial growth of $MgFe_2O_4$ (111) thin films on sapphire (0001) substrate. *Mater. Lett.* **65**, 3058–3060 (2011).
12. Cheng, J., Lazarov, V. K., Sterbinsky, G. E. & Wessels, B. W. Synthesis, structural and magnetic properties of epitaxial $MgFe_2O_4$ thin films by molecular beam epitaxy. *J. Vac. Sci. Technol. B* **27**, 148 (2009).
13. Lee, D. S. *et al.* The magnetic properties of strained and relaxed $Fe_{3-x}Mg_xO_4$ ferrite films on MgO(001) and $SrTiO_3$(001) by molecular beam epitaxy. *J. Appl. Phys.* **101**, 09M523 (2007).
14. Margulies, D. T. *et al.* Origin of the Anomalous Magnetic Behavior in Single Crystal Fe_3O_4 Films. *Phys. Rev. Lett.* **79**, 5162 (1997).
15. Margulies, D. T. *et al.* Anomalous moment and anisotropy behavior in Fe_3O_4 films. *Phys. Rev. B* **53**, 9175 (1996).
16. Eerenstein, W., Hibma, T. & Celotto, S. Mechanism for superparamagnetic behavior in epitaxial Fe_3O_4 films. *Phys. Rev. B* **70**, 184404 (2004).
17. Voogt, F. C. *et al.* Superparamagnetic behavior of structural domains in epitaxial ultrathin magnetite films. *Phys. Rev. B* **57**, R8107 (1998).
18. Arora, S. K. *et al.* Giant magnetic moment in epitaxial Fe_3O_4 thin films on MgO(100). *Phys. Rev. B* **77**, 134443 (2008).
19. Arora, S. K., Sofin, R. G. S. & Shvets, I. V. Magnetoresistance enhancement in epitaxial magnetite films grown on vicinal substrates. *Phys. Rev. B* **72**, 134404 (2005).
20. Eerenstein, W., Palstra, T. T. M., Saxena, S. S. & Hibma, T. Spin-polarized transport across sharp antiferromagnetic boundaries. *Phys. Rev. Lett.* **88**, 247204 (2002).
21. Wu, H. C. *et al.* Probing One Antiferromagnetic Antiphase Boundary and Single Magnetite Domain Using Nanogap Contacts. *Nano Lett.* **10**, 1132 (2010).
22. Wu, H. C. *et al.* Transversal magneto-resistance in epitaxial Fe_3O_4 and Fe_3O_4/NiO exchange biased system. *Appl. Phys. Lett.* **101**, 052402 (2012).
23. Jiang, J. C., Lin, Y., Chen, C. L., Chu, C. W. & Meletis, E. I. Microstructures and surface step-induced antiphase boundaries in epitaxial ferroelectric $Ba_{0.6}Sr_{0.4}TiO_3$ thin film on MgO. *J. Appl. Phys.* **91**, 3188 (2002).
24. He, J. *et al.* Twin-coupled domain structures in epitaxial relaxor ferroelectric Ba(Zr,Ti)O3 thin films on (001) MgO substrate. *Phil. Mag. Lett.* **89**, 493 (2009).

25. Venzke, S. *et al.* Epitaxial growth and magnetic behavior of $NiFe_2O_4$ thin films. *J. Mater. Res.* **11**, 1187 (1996).
26. Eerenstein, W., Celotto, S., Palstra, T. T. M. & Hibma, T. Diffusive motion of antiphase domain boundaries in Fe_3O_4 films. *Phys. Rev. B* **68**, 014428 (2003).
27. Ruiz-Zepeda, F. *et al.* Nanodomain induced anomalous magnetic and electronic transport properties of $LaBaCo_2O_{5.5+\delta}$ highly epitaxial thin films. *J. Appl. Phys.* **115**, 024301 (2014).
28. Liu, M., Ma, C. R., Enriquez, E., Xu, X., Bao, S. Y. & Chen, C. L. Effect of Annealing Ambient on Electrical Properties of $LaBaCo_2O_{5.5+\delta}$ Thin Films. *J. Nano Res.* **27**, 25 (2014).

Acknowledgments

This work was supported by Beijing Institute of Technology Research Fund Program for Young Scholars, Science Foundation of Ireland (SFI) under Contract No. 06/IN.1/I91, National Plan for Science and technology (Nos. NPST 1598-02 and NPST 1466-02) of King Abdulaziz City for Science and Technology. H.C.W., MA.A., and MO.A. thank Saudi Aramco for the financial support (project No. 6600028398). O. M. and A. S. acknowledge the financial support by the Bolashak Program funded by the Kazakhstan government.

Author contributions

H.C.W. and MOH.A. conceived the study. O.M., A.S. and C.C. grew the sample. H.C.W. performed the magnetic and transport measurements. A.K., A.M. and H.Z.Z. carried out the STEM measurements. MOU. A. and I.V.S. gave scientific advice. H.C.W. wrote the manuscript. All authors discussed the results and commented on the manuscript.

Additional information

Competing financial interests: The authors declare no competing financial interests.

How to cite this article: Wu, H.-C. *et al.* Magnetic and transport properties of epitaxial thin film $MgFe_2O_4$ grown on MgO (100) by molecular beam epitaxy. *Sci. Rep.* **4**, 7012; DOI:10.1038/srep07012 (2014).